Biophysical Journal
Article

Biophysical Society

Regulation of epithelial sodium channel activity by SARS-CoV-1 and SARS-CoV-2 proteins

Stephen N. Grant[1] and Henry A. Lester[2,*]
[1]Division of Chemistry and Chemical Engineering, Pasadena, California and [2]Division of Biology and Biological Engineering, California Institute of Technology, Pasadena, California

ABSTRACT Severe acute respiratory syndrome (SARS) coronavirus (CoV) 2 (SARS-CoV-2), which causes the coronavirus disease 2019, encodes several proteins whose roles are poorly understood. We tested their ability either to directly form plasma membrane ion channels or to change functions of two mammalian plasma membrane ion channels, the epithelial sodium channel (ENaC) and the $\alpha 3\beta 4$ nicotinic acetylcholine receptor. In mRNA-injected *Xenopus* oocytes, none of nine SARS-CoV-2 proteins or two SARS-CoV-1 proteins produced conductances, nor did co-injection of several combinations. Immunoblots for ORF8, spike (S), and envelope (E) proteins revealed that the proteins are expressed at appropriate molecular weights. In experiments on coexpression with ENaC, three tested SARS proteins (SARS-CoV-1 E, SARS-CoV-2 E, and SARS-CoV-2 S) markedly decrease ENaC currents. SARS-CoV-1 S protein decreases ENaC currents modestly. Coexpressing the E proteins but not the S proteins with $\alpha 3\beta 4$ nicotinic acetylcholine receptors significantly reduces acetylcholine-induced currents. ENaC inhibition does not occur if the SARS-CoV protein mRNAs are injected 24 h after the ENaC mRNAs, suggesting that SARS-CoV proteins affect early step(s) in functional expression of channel proteins. Consistent with the hypothesis that the SARS-CoV-2 S protein-induced ENaC inhibition involves competition for available protease, mutating the furin cleavage site in SARS-CoV-2 S protein partially relieves inhibition of ENaC currents. Extending previous suggestions that SARS proteins affect ENaC currents via protein kinase C (PKC) activation, PKC activation via phorbol 12-myristate 13-acetate decreases ENaC and $\alpha 3\beta 4$ activity. Phorbol 12-myristate 13-acetate application reduced membrane capacitance ~5%, presumably via increased endocytosis, but this decrease is much smaller than the SARS proteins' effects on conductances. Also, incubating oocytes in Gö-6976, a PKCα and PKCβ inhibitor, did not alter E or S protein-induced channel inhibition. We conclude that SARS-CoV-1 and SARS-CoV-2 proteins alter the function of human plasma membrane channels, via incompletely understood mechanisms. These interactions may play a role in the coronavirus 2019 pathophysiology.

SIGNIFICANCE The coronavirus 2019 pandemic has challenged all public health systems, and we are still in the early stages of understanding this disease and the virus that causes it, severe acute respiratory syndrome (SARS) coronavirus (CoV) 2. We know that respiratory distress is a primary symptom and one of the major causes of death in patients with the coronavirus 2019. Pulmonary edema is responsible for some of this stress. Pulmonary edema may result from improper epithelial sodium channel activity. SARS-CoV-1 envelope, SARS-CoV-2 envelope, and SARS-CoV-2 spike protein decrease epithelial sodium channel activity. This effect may play a role in disease progression, and the relationship between the SARS proteins and endogenous membrane channels may be clinically relevant and reveal therapeutic opportunities.

INTRODUCTION

The coronavirus disease 2019 (COVID-19) has caused a massive global public health crisis. As of 19 April 2021, over 140 million people have been infected and over three million lives have been lost to COVID-19, according to the Johns Hopkins Coronavirus Resource Center. The pandemic has spurred drastic changes throughout the world in every part of life. Understanding this virus gives the global community its best chance to return to relatively standard practices. However, much like the pandemic it elicited, severe acute respiratory syndrome (SARS) coronavirus (CoV) 2 is an unprecedented virus that requires study from various approaches.

We sought to contribute to COVID-19 research by systematically studying membrane-relevant SARS-CoV-2

Submitted December 15, 2020, and accepted for publication June 3, 2021.
*Correspondence: lester@caltech.edu
Editor: Henry Colecraft.
https://doi.org/10.1016/j.bpj.2021.06.005

proteins, both by themselves and in various combinations with host proteins, and comparing homologous proteins from SARS-CoV-1 and SARS-CoV-2. Plasma membrane viroporins are important for many viruses (1–5), and we tested for their presence in SARS-CoV-2 by expressing SARS-CoV-1 and SARS-CoV-2 proteins in *Xenopus* oocytes.

It is important to understand how the various proteins encoded by SARS-CoV-2 interact with endogenous human proteins (2,6,7). SARS-CoV-2 must interact with host proteins to replicate (8). These interactions begin when the SARS-CoV-2 spike (S) protein binds to the human angiotensin-converting enzyme 2 (ACE2) protein; this interaction leads to viral entry (9–11). Many subsequent interactions have been studied between SARS-CoV-2 and human proteins. Studies using mass spectrometry and in silico methods identified many protein-protein interactions between SARS-CoV-2 and humans (7,12). Additionally, researchers have looked to work done on SARS-CoV-1, the related β-coronavirus responsible for the SARS epidemic in 2002 and 2003 (13).

We are also interested in how the envelope (E) and S proteins from SARS-CoV-2 affect epithelial sodium channel (ENaC) function. Ji et al. (14) used electrophysiology to suggest that both SARS-CoV-1 E and S proteins markedly decreased ENaC activity in *Xenopus laevis* oocytes. After pharmacological experiments to probe the cause of this inhibition, Ji et al. (14) suggested that the E and S protein decreased ENaC protein levels via a protein kinase C (PKC)-dependent mechanism. ENaC helps regulate fluid levels in the lung, and if this function is inhibited, pulmonary edema can develop (15). Pulmonary edema has been observed in COVID-19 patients, so inhibition of ENaC via E and S protein expression may have been conserved in SARS-CoV-2 (16,17). Other ion channels may be affected by SARS-CoV-2 proteins, so we tested the generality of our results by studying how the SARS-CoV-1 and SARS-CoV-2 proteins affect $\alpha3\beta4$ nicotinic acetylcholine receptor (nAChR) activity. Finally, we begin mechanistic work to explain how the SARS-CoV-1 and SARS-CoV-2 proteins affect ENaC and $\alpha3\beta4$ nAChR currents.

MATERIALS AND METHODS

cDNA and mRNA

Human ENaC subunit cDNAs h-α-ENaC, h-β-ENaC, and h-γ-ENaC Myc were gifts from Christie Thomas (18). pLVX-EF1α-SARS-CoV-2-orf8-2xStrep-IRES-Puro, pLVX-EF1α-SARS-CoV-2-nsp2-2xStrep-IRES-Puro, pLVX-EF1α-SARS-CoV-2-nsp4-2xStrep-IRES-Puro, pLVX-EF1α-SARS-CoV-2-orf3a-2xStrep-IRES-Puro, and pLVX-EF1α-SARS-CoV-2-M-2xStrep-IRES-Puro were gifts from Nevan Krogan (7). pDONR223 SARS-CoV-2 NSP6 and pDONR207 SARS-CoV-2 NSP3 were gifts from Fritz Roth. pUC57-2019-nCoV-S plasmid was purchased from MolecularCloud (Piscataway, NJ). pcDNA3.1-SARS-Spike was a gift from Fang Li (19). The SARS-CoV-2 E protein plasmid was constructed and packaged by VectorBuilder (Chicago, IL). The vector identifier, VB200324-4348fzb, provides information about the vector on vectorbuilder.com. SARS-CoV-1 E protein was produced by introducing point mutations in the SARS-CoV-2 E protein plasmid. All SARS-CoV-1 and SARS-CoV-2 proteins were cloned into the pGEMHE vector for optimal *Xenopus* oocyte expression. The mouse $\alpha3$ and $\beta4$ nAChR mRNA have been described previously (20). mRNA was produced using the mMessage mMachine T7 Transcription Kit (Invitrogen, Waltham, MA) and purified with the RNeasy Mini Kit (QIAGEN, Hilden, Germany).

Protein expression in oocytes

X. laevis stage V and VI oocytes were harvested via standard protocols (21). For each ENaC subunit, 12 ng of mRNA was injected into oocytes. For mouse $\alpha3\beta4$ nAChR expression, 10 ng of mRNA for each subunit was injected into each oocyte. For the SARS-CoV-1 or SARS-CoV-2 proteins, 20 ng of mRNA was injected into oocytes along with the ENaC or $\alpha3\beta4$ nAChR mRNA. For oocytes injected with a single SARS-CoV-2 protein mRNA, each oocyte received 20 ng of mRNA. For oocytes injected with nine SARS-CoV-2 and two SARS-CoV-1 protein mRNA, 3 ng of each was injected into each oocyte. The final mRNA injection took place 24 h before electrophysiological recording or 48 h before lysis for immunoblotting.

Immunoblotting

48 h postinjection, oocyte lysates were prepared by lysing oocytes osmotically in a 20 mM HEPES (pH 7.3) solution (20 μl per oocyte) (22). Lysates were centrifuged for 5 min at 10,000 rpm. The supernatant was used to probe for E protein. The pellets were resuspended in 50 mM Tris, 150 mM NaCl, 1% NP-40 (pH 7.3) buffer, and these solutions were used to probe for ORF8 and S protein. 12% Mini-PROTEAN TGX Precast Protein Gels (Bio-Rad Laboratories, Hercules, CA) were used for electrophoresis and wet-transferred onto an Immun-Blot LF PVDF Membrane (Bio-Rad Laboratories, Hercules, CA). E protein was probed using rabbit antiserum that responds to the C-terminus of SARS-CoV-1 E protein at 1:1000 concentration. The antiserum was a gift from Carolyn Machamer (23). The ORF8 was probed using a primary antibody at 1:500 concentration (catalog number (Cat#): GTX135591; GeneTex, Irvine, CA). S protein was probed using a primary antibody at 1:500 concentration (Cat#: PA581795; Invitrogen, Waltham, MA). The primary antibodies were visualized using IRDye 800CW Donkey anti-Rabbit antibody (Cat#: 926-32213; Li-COR, Lincoln, NE) at 1:1000 concentration.

Electrophysiology

Oocyte recordings were performed in two-electrode voltage-clamp mode using the OpusXpress 6000A instrument (Axon Instruments, San Jose, CA). Oocyte equilibration and washes were performed with ND96 (96 mM NaCl, 2 mM KCl, 1.8 mM $CaCl_2$, 1 mM $MgCl_2$, and 5 mM HEPES (pH 7.4)) or High K^+ buffer (2 mM NaCl, 96 mM KCl, 1.8 mM $CaCl_2$, 1 mM $MgCl_2$, and 5 mM HEPES (pH 7.4)). Microelectrodes were fabricated from borosilicate glass (BF150-117-15; Sutter Instrument, Novato, CA) using a one-stage horizontal pull (P-87; Sutter Instrument, Novato, CA) and filled with 3 M KCl. Pipette resistances ranged from 0.3 to 3.0 MΩ. The initial holding potential was +10 mV for ENaC-expressing oocytes or −60 mV for $\alpha3\beta4$-expressing oocytes. For ENaC-expressing oocytes, voltages were sampled from −120 to +70 mV at 10 mV intervals, and the currents through the oocyte membrane were recorded. For $\alpha3\beta4$-expressing oocytes, the potential was held at −60 mV throughout the experiment, and the currents were measured during 100 μM acetylcholine (ACh) application. Data were sampled at 50 Hz. Traces were processed in Clampfit 11.1. In ENaC-expressing oocytes, amiloride-sensitive currents were calculated by subtracting currents measured in the presence of 10 μM amiloride

(an ENaC inhibitor) from the average currents measured in ND96 taken before amiloride treatment and after amiloride wash-out. For phorbol 12-myristate 13-acetate (PMA) experiments, oocyte currents were measured before and after 15 min incubation in the vehicle or 10 μM PMA. For Gö-6976 experiments, the oocytes were incubated in 1 μM Gö-6976 right after injection until electrophysiology experiments were performed.

Analysis and curve fitting was performed using Prism (GraphPad Software, La Jolla, CA). For the ENaC experiments in Figs. 3, 5, 6, 7, and 8, we fitted a second-order polynomial to each current-voltage data set (>10 oocytes, except where noted), to account for the nonlinear ENaC conductance. For control currents (for instance, co-injection with ORF8), the reversal potential (V_0) varied <5 mV within each experiment; however, the much smaller currents resulting from co-injection of other SARS-Cov-1 and SARS-CoV-2 proteins vitiated a meaningful estimate of V_0. The data plots show the 95% confidence limits of these fitting functions at each voltage between −120 and +70 mV. "Significant differences" between current-voltage relations in a particular voltage range mean that the 95% confidence limits do not overlap in that voltage range. This presentation has the following physiological and pathophysiological relevance: 1) that ENaC is expressed primarily in epithelial cells, a likely site of SARS-Cov-2 infection and proliferation (24–26), and 2) where possible, we extend the analysis to the >−60 mV resting potentials typical of epithelial cells.

Membrane capacitance was measured on oocytes for each voltage jump. The capacitive charge ΔQ was calculated by temporally integrating the transient capacitive current ($\Delta Q = \int \Delta I$) during the 20 ms after the command voltage jump. Fig. 3, *A* and *C* show how relatively large conductive currents challenge the voltage-clamp circuitry, the current amplifier's compliance, and the linearity of the current electrode so that ΔQ becomes distorted by the presence of a large conductance. An example of the resulting artifact is our lab's erroneous overestimate of the decreases in oocyte capacitance that accompany large decreases in K^+ currents (27). To minimize such artifacts in these experiments, we measured capacitance during the blockade of most ENaC currents by amiloride (10 mM). We also subtracted the remaining time-independent conductive currents by extrapolating such currents back to the time of the jump in the command voltage. We verified that the capacitive transient ΔQ showed a linear dependence on the voltage jump ΔV, allowing us to measure $C = \Delta V/\Delta Q$.

In analyses of data that emphasized currents at a single potential, an unpaired *t*-test was used to determine statistical significance between results with ORF8 co-injection versus each other co-injection (Fig. 4). A *p*-value of 0.05 or less was considered to be statistically significant.

RESULTS

SARS-CoV proteins do not form ion channels in the plasma membrane

Many viruses rely on the function of viroporins, including viruses in the coronavirus family (2,4,6,23,28). The ORF3a and E protein are postulated to be viroporins (29). Furthermore, there are viral protein-protein interactions such that the individual protein does not create a pore, but together they do so (30). Here, we find that the injection of SARS-CoV-1 S and E and SARS-CoV-2 Nsp2, Nsp3, Nsp4, Nsp6, ORF3a, ORF8, M, E, and S protein mRNA, all simultaneously or individually, into *Xenopus* oocytes does not produce conductances in the plasma membrane (Fig. 1).

SARS proteins are expressed after mRNA injection

Although most properly transcribed mRNA is translated into proteins when injected into oocytes, there are exceptions. Here, we made immunoblots to determine whether a subset of these SARS proteins are translated in oocytes. We specifically studied the S, E, and SARS-CoV-2 ORF8 proteins. Each SARS protein was only observed in oocytes injected with their respective mRNA (Fig. 2). These results suggest that S, E, and SARS-CoV-2 ORF8 proteins are expressed in the oocytes after mRNA injection; inadequate protein translation or protein degradation does not underlie the lack of plasma membrane conductances.

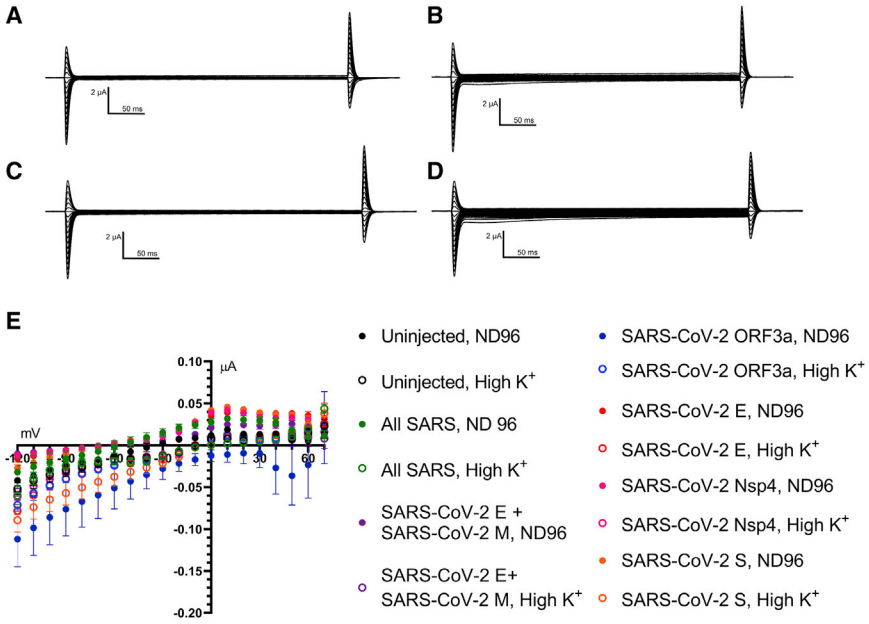

FIGURE 1 SARS-CoV-1 and SARS-CoV-2 mRNA do not produce conductances in the plasma membrane of *Xenopus* oocytes. (*A–D*) Voltage-clamp traces for steps from a holding potential of +10 mV to various test potentials between −120 and +70 mV. (*A*) "All SARS" (oocytes injected with SARS-CoV-1 S, SARS-CoV-1 E, and SARS-CoV-2 Nsp2, Nsp3, Nsp4, Nsp6, ORF3a, ORF8, M, E, and S protein mRNA) oocytes in ND96 buffer. (*B*) "All SARS" oocytes in high K^+ buffer. (*C*) Uninjected oocytes in ND96 buffer. (*D*) Uninjected oocytes in high K^+ buffer. (*E*) Current-Voltage (I-V) relationship for all samples with error bars representing the mean ± SE. n = 12 (All SARS in ND96), 13 (All SARS in High K^+), 5 (uninjected in ND96), 11 (uninjected in High K^+), 18 (ORF3a ND96), 43 (ORF3a, High K^+), 8 (E + M, ND96), 8 (E + M, High K^+), 37 (Nsp4, ND96), 45 (Nsp4, High K^+), 15 (E, ND96), 23 (E, High K^+), 64 (S, ND96), and 19 (S, High K^+).

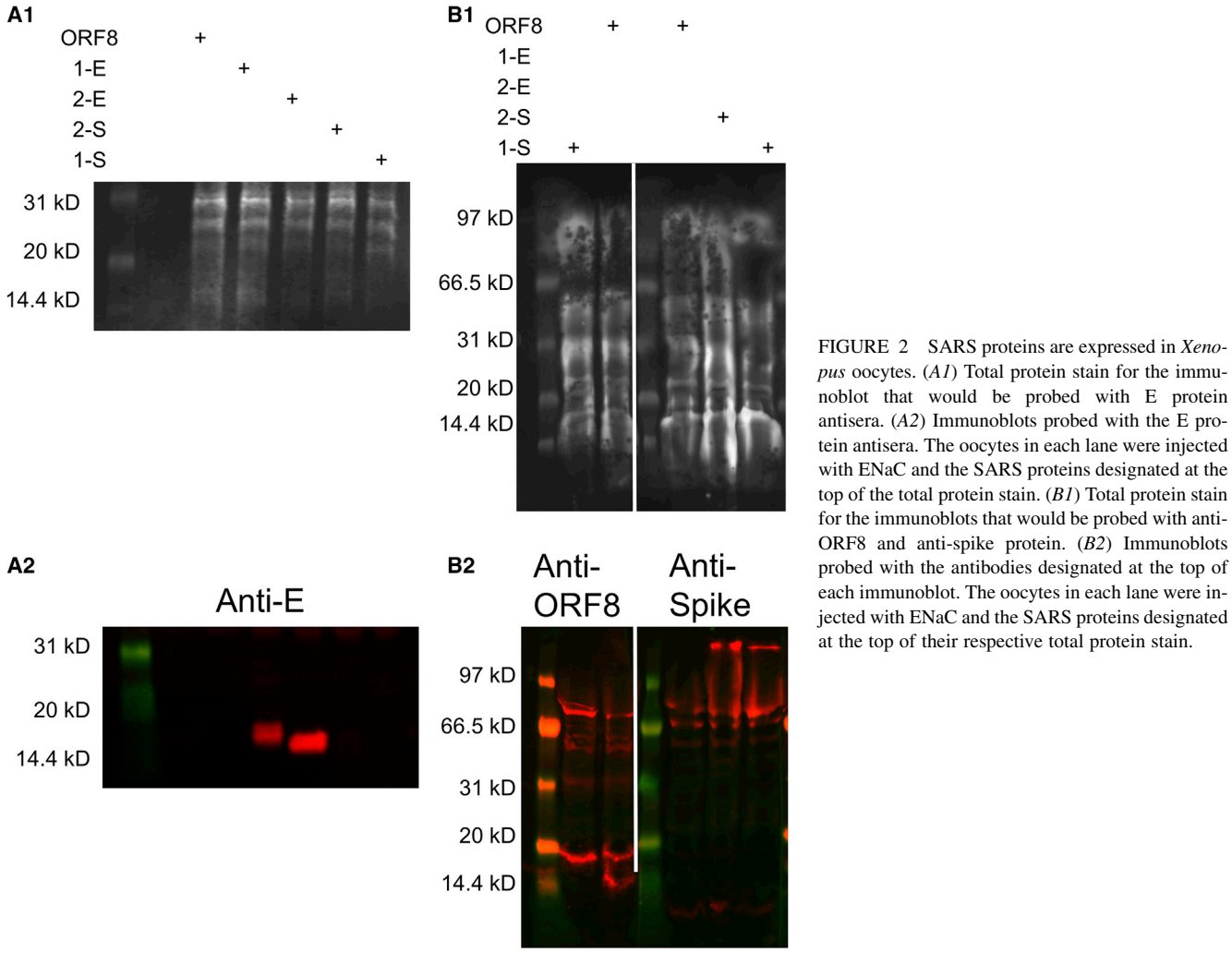

FIGURE 2 SARS proteins are expressed in *Xenopus* oocytes. (*A1*) Total protein stain for the immunoblot that would be probed with E protein antisera. (*A2*) Immunoblots probed with the E protein antisera. The oocytes in each lane were injected with ENaC and the SARS proteins designated at the top of the total protein stain. (*B1*) Total protein stain for the immunoblots that would be probed with anti-ORF8 and anti-spike protein. (*B2*) Immunoblots probed with the antibodies designated at the top of each immunoblot. The oocytes in each lane were injected with ENaC and the SARS proteins designated at the top of their respective total protein stain.

SARS-CoV-1 E, SARS-CoV-2 E, and SARS-CoV-2 S proteins decrease ENaC currents

Protein-protein interactions between the virus and host are crucial for viral entry, replication, maturation, transport, and secretion. Ji et al. (14) investigated the SARS-CoV-1 E and S protein interactions with ENaC. Here, we repeated these experiments and included the SARS-CoV-2 proteins (Fig. 3). We use SARS-CoV-2 ORF8 as a negative control plasmid because ORF8 does not produce viroporins in the plasma membrane and is not expected to interact with ENaC (29). Compared to oocytes injected with ORF8, oocytes injected with SARS-CoV-1 E, SARS-CoV-2 E, and SARS-CoV-2 S protein decrease ENaC currents, with the E proteins having a greater effect than SARS-CoV-2 S protein. Furthermore, we find that SARS-CoV-2 E protein inhibits ENaC more than SARS-CoV-1 E protein. Although Ji et al. (14) report that SARS-CoV-1 S protein also decreases ENaC current, we find that this is true compared with oocytes injected only with ENaC, the control Ji et al. used. However, when the control is oocytes co-injected with ORF8, there is no significant difference between oocytes co-injected with SARS-CoV-1 S or the control mRNA. Altogether, we find that the E and S protein from SARS-CoV-2 have a greater inhibitory effect on ENaC than their SARS-CoV-1 counterparts.

The SARS-CoV-1 and -2 E proteins differ at two sequence regions, positions 55–56 and 69–70. We constructed two chimera-like E proteins in which either the 55–56 or 69–70 sequences differ, but not both. Proteins with the SARS-CoV-1 E protein residues at 69–70 are one amino acid longer than proteins with the SARS-CoV-2 E protein residues at 69–70 because this sequence is Glu-Gly in SARS-CoV-1 and Arg-(Δ) in SARS-CoV-2. Like both unmutated E proteins, both of these chimera-like proteins markedly decreased ENaC current.

SARS-CoV-1 and SARS-CoV-2 E protein inhibit $\alpha 3\beta 4$ nAChR currents

Next, we were interested in the SARS proteins' general effect on ion channels. We studied the $\alpha 3\beta 4$ nAChR because it

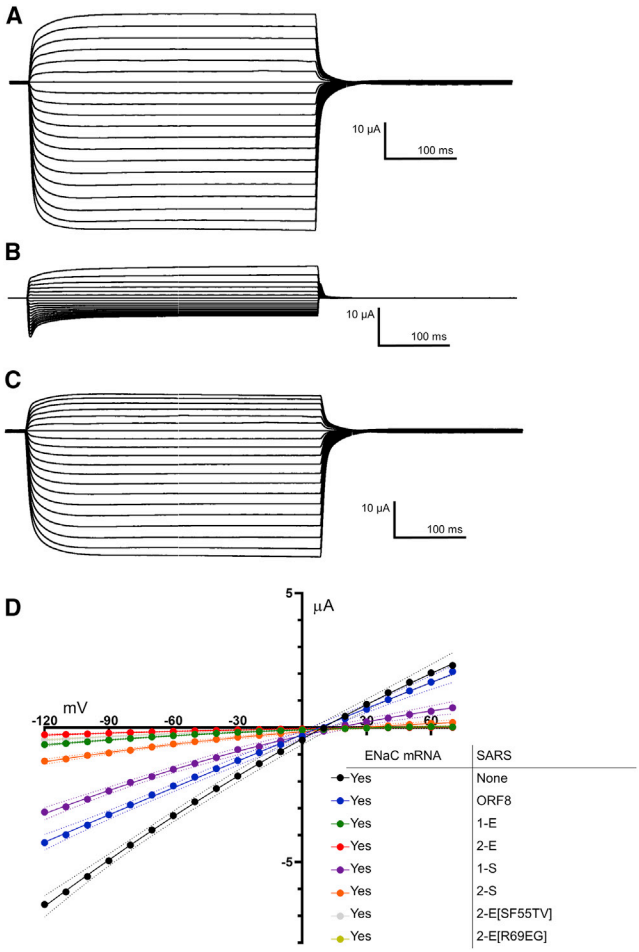

FIGURE 3 Representative voltage-clamp currents. Membrane potential was held at +10 mV, then stepped to test potentials from −120 to +70 mV at 10 mV intervals. (*A*) Buffer. (*B*) 10 μM amiloride. (*C*) Subtraction of the amiloride traces from the buffer traces, producing the amiloride-sensitive currents and used to determine ENaC currents. (*D*) I-V relationships for oocytes injected with ENaC mRNA and SARS proteins. ORF8, SARS-CoV-2 ORF 8; 1-E, SARS-CoV-1 E protein; 2-E, SARS-CoV-2 E protein; 2-S, SARS-CoV-2 S protein; 1-S, SARS-CoV-1 S protein. "2-E[SF55TV]" refers to the chimera-like E protein with the partial P**TV**YVYSRVKNLNSS**R**-V sequence. "2-E[R69EG]" refers to the chimera-like E protein with the partial P**SF**YVYSRVKNLNSS**EG**V sequence (this protein is one amino acid longer than wild-type SARS-CoV-2 E protein). The dotted line represents the 95% confidence interval. n = 18 (ENaC only), 49 (ORF8), 52 (1-S), 51 (2-S), 35 (1-E), 40 (2-E), 30 (2-E[SF55TV]), and 30 (2-E[R69EG]).

is readily expressed in *Xenopus* oocytes and plays a role in several respiratory diseases (31). Once again, we find that $\alpha 3\beta 4$ currents are significantly reduced when oocytes are co-injected with either E protein (Fig. 4). However, in contrast to our ENaC experiments, SARS-CoV-2 S protein does not significantly reduce $\alpha 3\beta 4$ currents.

Inhibition does not occur if the SARS-CoV protein mRNAs are injected 24 h after ENaC mRNA

The individual ENaC subunits must be translated, folded, assembled into mature channels, and trafficked to the

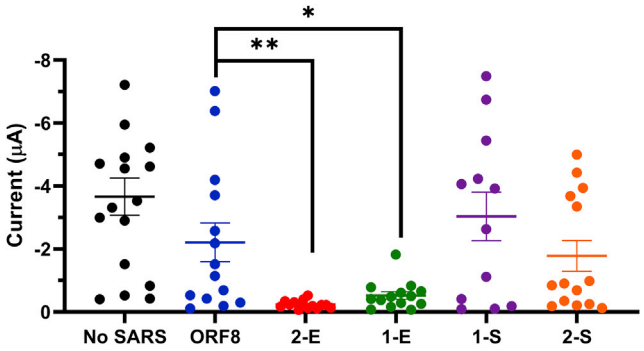

FIGURE 4 Currents induced by 100 μM ACh in oocytes expressing mouse $\alpha 3\beta 4$ and SARS mRNA. ORF8, SARS-CoV-2 ORF 8; 1-E, SARS-CoV-1 E protein; 2-E, SARS-CoV-2 E protein; 2-S, SARS-CoV-2 S protein; 1-S, SARS-CoV-1 S protein. The error bars represent the mean ± SE. *p*-values were calculated from an unpaired *t*-test, where * denotes $p < 0.05$ and ** denotes $p < 0.005$.

plasma membrane. ENaC currents are observed 24 h after mRNA injection, suggesting that these steps occur within that time. To understand whether the SARS-CoV proteins affect ENaC during these steps, we injected ENaC mRNA and waited 24 h before injecting the SARS-CoV mRNA. We find that if the SARS-CoV mRNA is injected 24 h after the ENaC mRNA, there is no ENaC inhibition (Fig. 5).

We interpret the experiment of Fig. 5 as follows. On the one hand, delaying ORF8 injection by 24 h significantly increases ENaC conductance by 2–3 fold, at $V < -30$ mV and $V > +40$ mV. This effect may indicate that ORF8 inhibits ENaC expression or function modestly during the first

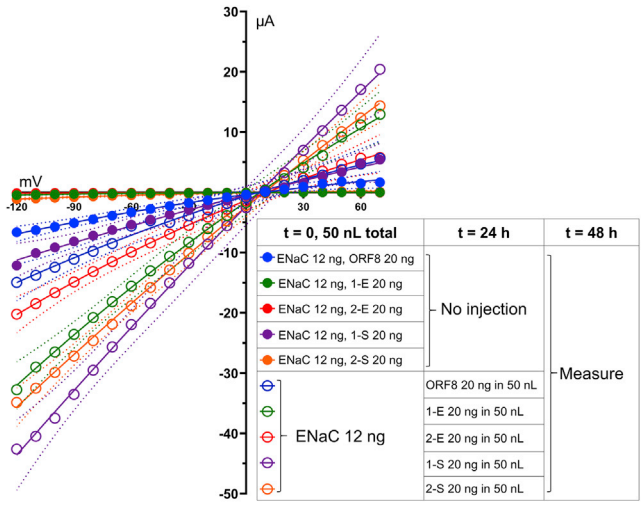

FIGURE 5 Injecting oocytes with the SARS mRNA 24 h after ENaC mRNA injection does not result in ENaC inhibition. The filled circles represent samples for which both ENaC and SARS mRNA were injected at the same time. The open circles represent samples that had the SARS mRNA injected after the ENaC mRNA. The dotted line represents the 95% confidence interval. n = 4 (48 h (ENaC + ORF8)), 12 (48 h (ENaC + 1-E)), 13 (48 h (ENaC + 2-E)), 8 (48 h (ENaC + 1-S)), 11 (48 h (ENaC + 2-S)), 6 (ENaC then ORF8), 8 (ENaC then 1-E), 10 (ENaC then 10), 5 (ENaC then 1-S), and 6 (ENaC then 2-S).

24 h after co-injection. On the other hand, delaying the SARS-CoV-2 S protein, SARS-CoV-1 E protein, or SARS-CoV-2 E protein mRNA injection by 24 h produces more dramatic increases. Quantitative comparisons are vitiated by the very small currents produced by co-injection; but the increase is >10-fold. Therefore, we conclude that the severe block of ENaC by SARS-CoV-1 E, SARS-CoV-2 S, or SARS-CoV-2 E proteins all occur at early steps in the functional expression of channel proteins. The relatively modest block by SARS-CoV-1 S protein presents an intermediate case. Delaying SAR-CoV-1 S co-injection by 24 h produces a ~4-fold increase in ENaC conductance when measured at all voltages outside the −20 to +20 mV range.

Mutating the furin cleavage site in SARS-CoV-2 S protein improves ENaC function

ENaC function is dependent on a furin cleavage event, whereas $\alpha 3\beta 4$ does not depend on furin cleavage (32). The ability of SARS-CoV-2 S protein to inhibit ENaC but not $\alpha 3\beta 4$ could be explained by the furin cleavage site in SARS-CoV-2 S protein that may compete for available furin. Indeed, several others have proposed this mechanism for possible ENaC inhibition via SARS-CoV-2 S protein expression (33–35). We mutated the ^{682}RRAR^{685} motif to ^{682}AAAR^{685} to destroy the furin cleavage site. In oocytes expressing ENaC, there was greater current when we expressed the SARS-CoV-2 S [^{682}AAAR^{685}] mutant instead of the wild-type SARS-CoV-2 S protein (Fig. 6). However, the currents were not completely restored, suggesting that other factors influence ENaC inhibition by SARS-CoV-2 S protein.

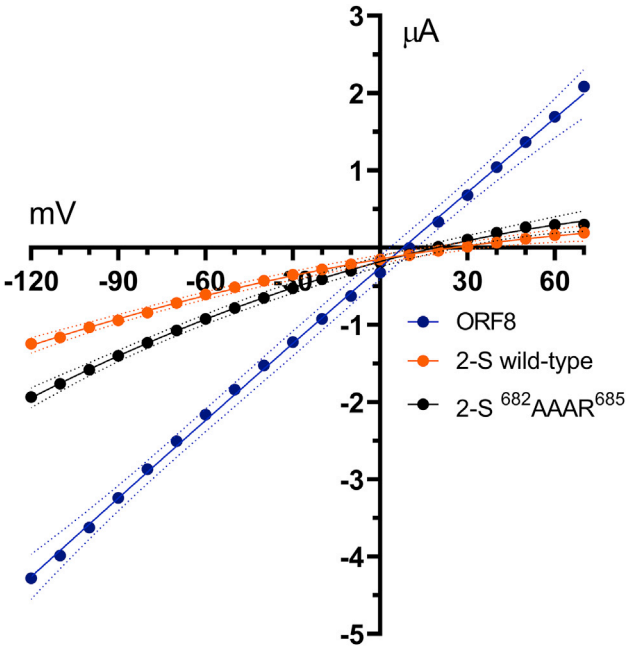

FIGURE 6 Mutating the SARS-CoV-2 S protein furin cleavage site (^{682}RRAR^{685}) to ^{682}AAAR^{685} improves ENaC function after co-injection. n = 49 (ORF8), 51 (2-S wild-type), and 30 (2-S ^{682}AAAR^{685}).The dotted line represents the 95% confidence interval.

PKC activation decreases ENaC and $\alpha 3\beta 4$ currents

PKC helps regulate many cellular functions, including net endocytosis (36). Ji et al. (14) suggested that PKC activation is the cause for decreased ENaC currents due to SARS-CoV-1 S or E protein expression. They hypothesized that as endocytosis occurs, the number of ENaC channels on the plasma membrane decrease, and the total ENaC current decreases pari passu (14). Here, we verify that PKC activation decreases ENaC and $\alpha 3\beta 4$ currents after 15 min of treatment in 10 μM PMA, a PKC activator (37). We find that compared with vehicle, currents are significantly lower after PMA treatment, consistent with the hypothesis of Ji et al. (14) that PKC activation decreases plasma membrane currents (Fig. 7). Additionally, based on our capacitance measurements, net endocytosis increased (membrane area decreased ~5%) after PMA treatment (Fig. S1).

PKC inhibition does not abolish SARS-CoV-1 E, SARS-CoV-2 E, or SARS-CoV-2 S protein-induced reductions in ENaC currents

We tried to inhibit PKC activation with Gö-6976, a known PKC inhibitor (38). We hypothesized that if we can prevent PKC activation with Gö-6976, then the effects of SARS-CoV-1 E, SARS-CoV-2 S, and SARS-CoV-2 E will be abolished. However, after incubating oocytes in 1 μM Gö-6976 after mRNA injection, we found no differences between Gö-6976-treated and vehicle-treated cells (Fig. 8). Once again, this is somewhat consistent with the data of Ji et al. (14) in that Gö-6976 treatment did not completely recover ENaC currents, although our data suggest a much less impressive improvement with Gö-6976 treatment. Nonetheless, both Ji et al. (14) and we suggest that, although PKC activation can decrease ENaC currents, the SARS proteins appear to be utilizing other mechanisms as well.

DISCUSSION

COVID-19 has wreaked havoc on the world in unprecedented ways. We show that the SARS-CoV-1 and SARS-CoV-2 proteins, expressed either singly or in combination, do not produce conductance at the plasma membrane (Fig. 1). This contrasts with reports suggesting that SARS-CoV-1 and SARS-CoV-2 may produce viroporins on the plasma membrane (39–41). We verify that proteins are being translated by detecting E, S, and ORF8 proteins via immunoblots (Fig. 2) and by observing inhibition of other channels. Whereas these results do not prove the absence of ion channels in other intracellular regions (5), the plasma membrane's lack of ion channels complicates some therapeutic strategies.

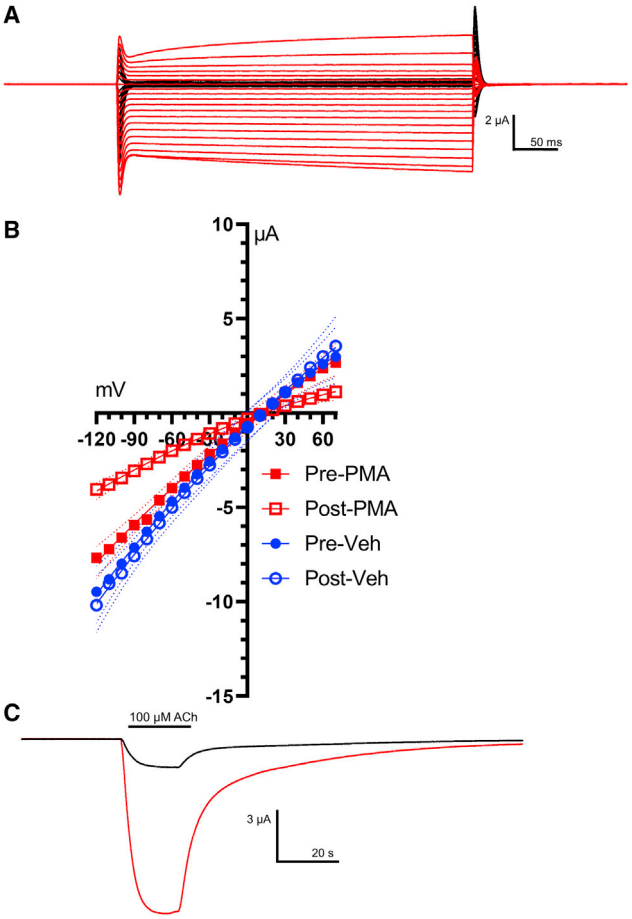

FIGURE 7 PKC activation via 10 μM PMA treatment decreases ENaC and $\alpha 3\beta 4$ currents. Oocyte currents were measured before (Pre-) and after (Post-) 15 min treatment with vehicle or 10 μM PMA. (*A*) Traces for oocytes expressing ENaC. Red traces represent before PMA ("Pre-PMA") and the black traces are after PMA ("Post-PMA"). This oocyte showed unusually large suppression of ENaC currents by PMA (*B*) I-V relationships for oocytes expressing ENaC before or after vehicle or PMA treatment. The dotted line represents the 95% confidence interval. n = 10 (Pre-Veh), 10 (Post-Veh), 12 (Pre-PMA), and 13 (Post-PMA). (*C*) Traces for oocytes expressing $\alpha 3\beta 4$; as noted by the horizontal bar, 100 μM ACh was present. Red traces represent before PMA ("Pre-PMA") and the black traces are after PMA ("Post-PMA").

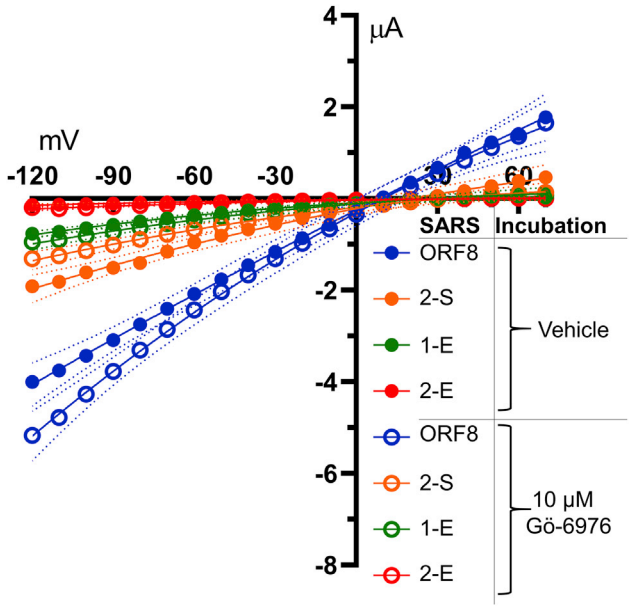

FIGURE 8 PKC inhibition with 1 μM Gö-6976 does not prevent E protein or SARS-CoV-2 S protein-related decreases in ENaC activity. For each co-injection, there is no significant difference between the oocytes treated with vehicle or Gö-6976. ORF8, SARS-CoV-2 ORF8; 1-E, SARS-CoV-1 E protein; 2-E, SARS-CoV-2 E protein; 2-S, SARS-CoV-2 S protein. The dotted line represents the 95% confidence interval. n = 11 (ORF Veh), 11 (1-E Veh), 12 (2-E Veh), 10 (2-S Veh), 14 (ORF8 plus Gö-6976), 13 (1-E plus Gö-6976), 7 (2-E plus Gö-6976), and 11 (2-S plus Gö-6976).

Caveats include that a *Xenopus*' oocytes differ markedly from human epithelial cells, so further work must be done on other model systems to produce a more comprehensive understanding of SARS-CoV-2 proteins' roles in COVID-19. Also, the intracellular life cycle of a coronavirus involves several steps in organelles; if the SAR-CoV proteins produce channels in organelles, these might not traffic to the plasma membrane and might therefore escape detection in our experiments.

As in many viral diseases, viral protein-host protein interactions underlie the pathophysiology of COVID-19. Therefore, we have studied interactions that include the effects of E or S protein expression on ENaC or $\alpha 3\beta 4$ activity. In SARS-CoV-1, Ji et al. (14) found that E and S protein expression decreased ENaC activity. Our observations suggest that the inhibitory properties are greater for the SARS-CoV-2 E protein and S protein (Fig. 3). We found that in $\alpha 3\beta 4$-expressing oocytes, both E proteins decreased $\alpha 3\beta 4$ currents (Fig. 4). For S protein, Ji et al. (14) found that SARS-CoV-1 S protein decreased ENaC activity. In contrast, our results suggest that SARS-CoV-2 S protein but not SARS-CoV-1 S protein has this effect. This difference is likely due to a difference in our control experiments. On the one hand, Ji et al. (14) compared their currents to samples only injected with ENaC; on the other hand, we compared our results to samples co-injected with ORF8, a protein that is not expected to interact with ENaC. Therefore, we hypothesize that the decreased ENaC currents that we observe for SARS-CoV-1 S protein (that do not significantly differ from samples injected with ORF8) are due to occlusion of translational or trafficking pathways (42) instead of a selective effect from the translated proteins. However, oocytes co-injected with SARS-CoV-2 S protein did have significantly lower ENaC currents compared with our controls. We show that the inhibitions do not occur if the SARS-CoV protein mRNAs are injected 24 h after ENaC mRNAs, suggesting that SARS-CoV proteins affect early step(s) in the functional expression of channel proteins (Fig. 5).

Previous studies show that some viral fusion proteins are activated by proteolysis (43). The increased inhibition with

SARS-CoV-2 S protein is consistent with the appearance of a furin cleavage site (44). This site is identical to the furin cleavage site in the ENaC-α subunit, so SARS-CoV-2 S protein may be competing for available furin, thereby decreasing the proteolytic activation of ENaC-α and thus decreasing ENaC activity (18,35,45). SARS-CoV-2 S protein competing for furin would also explain how $\alpha3\beta4$ currents do not change with SARS-CoV-2 S protein expression; $\alpha3\beta4$ does not depend on furin cleavage for activity. Our experiments with the SARS-CoV-2 S [^{682}AAAR^{685}] mutant support this hypothesis, although it does not completely explain SARS-CoV-2-induced ENaC inhibition because uninhibited ENaC currents were not observed (Fig. 6).

We hypothesized, similar to Ji et al. (14), that PKC activation may partly underlie the decreased currents. When PKC is activated, net endocytosis increases (36). Decreasing the number of channels on the membrane via endocytosis is expected to decrease currents. When we examined this relationship quantitatively in oocytes treated with PMA, we observed only a modest ($\sim$5%) decrease in membrane area (as a decrease in capacitance) along with a much larger decrease in membrane currents through ENaC and $\alpha3\beta4$ (Fig. 7; Fig. S1). Furthermore, when we blocked PKC activation with Gö-6976 treatment, we did not block the inhibitory effects of SARS-CoV-1 E, SARS-CoV-2 E, or SARS-CoV-2 S protein (Fig. 8). Although these SARS proteins may be activating PKC, there appear to be other mechanisms that inhibit ENaC activity as well.

Both chimera-like E protein constructs suppressed ENaC currents like the parent proteins. Although we could not directly probe events in the Golgi (where the E protein is expected to localize (46)), this result suggests that combining the two regions conferred no selective advantage to SARS-CoV-2, at least as measured by our assay of ENaC suppression. Among the presently known SARS-CoV-2 variant lineages, we have noted no mutations at the 55–56 and 69–70 positions. Several members of the B.1.351 lineage have a P71L mutation; this position is near the 69–70 sequence and immediately upstream from a candidate PDZ domain binding motif at the C-terminus.

CONCLUSIONS

Unfortunately, COVID-19 will not be the last virus to cross over into humans and strain public health resources. Although the COVID-19 vaccine will greatly help the world recover from this pandemic, basic research into SARS-CoV-2 will improve our response when the next viral infection emerges.

Because SARS and COVID-19 are different diseases, one expects to note differences between the proteins from SARS-CoV-1 and SARS-CoV-2. Here, we show that the E and S proteins inhibit ENaC and are more potent at inhibiting ENaC than their SARS-CoV-1 counterparts. ENaC participates in lung fluid homeostasis, so an improperly functioning ENaC may result in pulmonary edema (14,15). If ENaC is inhibited more in COVID-19 than in SARS, this may help us predict the course of future viral diseases. Indeed, if pulmonary edema is more prominent in COVID-19 patients than SARS patients, the different S and E proteins may be responsible. Additionally, the SARS-CoV-2 variants are troubling. Most researchers emphasize that any differential virulence or lethality of variant S proteins may arise via differential interactions with antibodies (induced either by host infection or by vaccines). This report presents quantitative data on another S protein effect: consequences of interactions with host non-antibody proteins. One such interaction, not studied here, is binding to the ACE2 receptor. Measuring the interactions made by the S and E proteins with human proteins may be crucial to understanding COVID-19 and the SARS-CoV-2 variants. We are still in the early stages of understanding SARS-CoV-2 and COVID-19. Although our findings may be meaningful and important, they represent only part of the required knowledge about SARS-CoV-2 and COVID-19.

SUPPORTING MATERIAL

Supporting material can be found online at https://doi.org/10.1016/j.bpj.2021.06.005.

AUTHOR CONTRIBUTIONS

S.N.G. designed and performed the experiments, analyzed the data, and prepared the manuscript. H.A.L. designed the experiments, analyzed the data, prepared the manuscript, and supervised the project.

ACKNOWLEDGMENTS

We thank Drs. Christopher Barnes, Bruce N. Cohen, Douglas Eaton, Carolyn Machamer, Gerhard Thiel, Anthony West, Nael McCarty, Dennis A. Dougherty and Nathan Dascal for useful insights, and Jonathan Wang for harvesting oocytes.

This work was supported by the National Institute of Drug Abuse (DA046122 and DA049140), the National Institute of General Medical Sciences (GM-123582), and the California Tobacco-Related Disease Program (29IR0445 to D.A. Dougherty).

REFERENCES

1. Zhang, R., K. Wang, …, B. Sun. 2014. The ORF4a protein of human coronavirus 229E functions as a viroporin that regulates viral production. *Biochim. Biophys. Acta.* 1838:1088–1095.
2. To, J., and J. Torres. 2018. Beyond channel activity: protein-protein interactions involving viroporins. *In* Subcellular Biochemistry. Virus Protein and Nucleoprotein Complexes. J. R. Harris and D. Bhella, eds. Springer, pp. 329–377.
3. Farag, N. S., U. Breitinger, …, M. A. El Azizi. 2020. Viroporins and inflammasomes: a key to understand virus-induced inflammation. *Int. J. Biochem. Cell Biol.* 122:105738.
4. Wang, C., K. Takeuchi, …, R. A. Lamb. 1993. Ion channel activity of influenza A virus M2 protein: characterization of the amantadine block. *J. Virol.* 67:5585–5594.

5. Cabrera-Garcia, D., R. Bekdash, …, N. L. Harrison. 2021. The envelope protein of SARS-CoV-2 increases intra-Golgi pH and forms a cation channel that is regulated by pH. *J. Physiol.* 599:2851–2868.
6. Torres, J., W. Surya, …, D. X. Liu. 2015. Protein-protein interactions of viroporins in coronaviruses and paramyxoviruses: new targets for antivirals? *Viruses.* 7:2858–2883.
7. Gordon, D. E., G. M. Jang, …, N. J. Krogan. 2020. A SARS-CoV-2 protein interaction map reveals targets for drug repurposing. *Nature.* 583:459–468.
8. Chen, Y., Q. Liu, and D. Guo. 2020. Emerging coronaviruses: genome structure, replication, and pathogenesis. *J. Med. Virol.* 92:418–423.
9. Yan, R., Y. Zhang, …, Q. Zhou. 2020. Structural basis for the recognition of SARS-CoV-2 by full-length human ACE2. *Science.* 367:1444–1448.
10. Wrapp, D., N. Wang, …, J. S. McLellan. 2020. Cryo-EM structure of the 2019-nCoV spike in the prefusion conformation. *Science.* 367:1260–1263.
11. Hoffmann, M., H. Kleine-Weber, …, S. Pöhlmann. 2020. SARS-CoV-2 cell entry depends on ACE2 and TMPRSS2 and is blocked by a clinically proven protease inhibitor. *Cell.* 181:271–280.e8.
12. Guzzi, P. H., D. Mercatelli, …, F. M. Giorgi. 2020. Master regulator analysis of the SARS-CoV-2/human interactome. *bioRxiv* https://doi.org/10.1101/2020.03.15.992925.
13. Ng, M. L., S. H. Tan, …, A. E. Ling. 2003. Proliferative growth of SARS coronavirus in Vero E6 cells. *J. Gen. Virol.* 84:3291–3303.
14. Ji, H. L., W. Song, …, S. Matalon. 2009. SARS-CoV proteins decrease levels and activity of human ENaC via activation of distinct PKC isoforms. *Am. J. Physiol. Lung Cell. Mol. Physiol.* 296:L372–L383.
15. Fronius, M. 2013. Treatment of pulmonary edema by ENaC activators/stimulators. *Curr. Mol. Pharmacol.* 6:13–27.
16. Valtueña, J., D. Ruiz-Sánchez, …, M. Garayar-Cantero. 2020. Acral edema during the COVID-19 pandemic. *Int. J. Dermatol.* 59:1155–1157.
17. Zwaveling, S., R. Gerth van Wijk, and F. Karim. 2020. Pulmonary edema in COVID-19: explained by bradykinin? *J. Allergy Clin. Immunol.* 146:1454–1455.
18. Raikwar, N. S., and C. P. Thomas. 2008. Nedd4-2 isoforms ubiquitinate individual epithelial sodium channel subunits and reduce surface expression and function of the epithelial sodium channel. *Am. J. Physiol. Renal Physiol.* 294:F1157–F1165.
19. Shang, J., G. Ye, …, F. Li. 2020. Structural basis of receptor recognition by SARS-CoV-2. *Nature.* 581:221–224.
20. Blom, A. E. M., H. R. Campello, …, D. A. Dougherty. 2019. Probing binding interactions of cytisine derivatives to the α4β2 nicotinic acetylcholine receptor. *J. Am. Chem. Soc.* 141:15840–15849.
21. Henderson, B. J., S. Grant, …, H. A. Lester. 2019. Menthol stereoisomers exhibit different effects on α4β2 nAChR upregulation and dopamine neuron spontaneous firing. *eNeuro.* 5.
22. Lin-Moshier, Y., and J. S. Marchant. 2013. A rapid Western blotting protocol for the Xenopus oocyte. *Cold Spring Harb. Protoc.* 2013.
23. Cohen, J. R., L. D. Lin, and C. E. Machamer. 2011. Identification of a Golgi complex-targeting signal in the cytoplasmic tail of the severe acute respiratory syndrome coronavirus envelope protein. *J. Virol.* 85:5794–5803.
24. Mulay, A., B. Konda, …, B. R. Stripp. 2021. SARS-CoV-2 infection of primary human lung epithelium for COVID-19 modeling and drug discovery. *Cell Rep.* 35:109055.
25. Melms, J. C., J. Biermann, …, B. Izar. 2021. A molecular single-cell lung atlas of lethal COVID-19. *Nature*, Published online April 29, 2021.
26. Delorey, T. M., C. G. K. Ziegler, …, A. Regev. 2021. COVID-19 tissue atlases reveal SARS-CoV-2 pathology and cellular targets. *Nature*, Published online April 29, 2021.
27. Tong, Y., G. S. Brandt, …, H. A. Lester. 2001. Tyrosine decaging leads to substantial membrane trafficking during modulation of an inward rectifier potassium channel. *J. Gen. Physiol.* 117:103–118.
28. Shimbo, K., D. L. Brassard, …, L. H. Pinto. 1995. Viral and cellular small integral membrane proteins can modify ion channels endogenous to Xenopus oocytes. *Biophys. J.* 69:1819–1829.
29. Castaño-Rodriguez, C., J. M. Honrubia, …, L. Enjuanes. 2018. Role of severe acute respiratory syndrome coronavirus viroporins E, 3a, and 8a in replication and pathogenesis. *MBio.* 9:e02325-17.
30. Wolff, G., R. W. A. L. Limpens, …, M. Bárcena. 2020. A molecular pore spans the double membrane of the coronavirus replication organelle. *Science.* 369:1395–1398.
31. Mazzo, F., F. Pistillo, …, S. F. Colombo. 2013. Nicotine-modulated subunit stoichiometry affects stability and trafficking of α3β4 nicotinic receptor. *J. Neurosci.* 33:12316–12328.
32. Harris, M., A. Garcia-Caballero, …, B. C. Rossier. 2008. Preferential assembly of epithelial sodium channel (ENaC) subunits in Xenopus oocytes: role of furin-mediated endogenous proteolysis. *J. Biol. Chem.* 283:7455–7463.
33. Anand, P., A. Puranik, …, V. Soundararajan. 2020. SARS-CoV-2 strategically mimics proteolytic activation of human ENaC. *eLife.* 9:e58603.
34. Gentzsch, M., and B. C. Rossier. 2020. A pathophysiological model for COVID-19: critical importance of transepithelial sodium transport upon airway infection. *Function (Oxf).* 1:a024.
35. Szabó, G. T., A. Kiss, …, D. Czuriga. 2021. Hypothetical dysfunction of the epithelial sodium channel may justify neurohumoral blockade in coronavirus disease 2019. *ESC Heart Fail.* 8:171–174.
36. Alvi, F., J. Idkowiak-Baldys, …, Y. A. Hannun. 2007. Regulation of membrane trafficking and endocytosis by protein kinase C: emerging role of the pericentrion, a novel protein kinase C-dependent subset of recycling endosomes. *Cell. Mol. Life Sci.* 64:263–270.
37. Vasilets, L. A., G. Schmalzing, …, W. Schwarz. 1990. Activation of protein kinase C by phorbol ester induces downregulation of the Na+/K(+)-ATPase in oocytes of *Xenopus laevis*. *J. Membr. Biol.* 118:131–142.
38. Martiny-Baron, G., M. G. Kazanietz, …, C. Schächtele. 1993. Selective inhibition of protein kinase C isozymes by the indolocarbazole Gö 6976. *J. Biol. Chem.* 268:9194–9197.
39. Sarkar, M., and S. Saha. 2020. Structural insight into the putative role of novel SARS CoV-2 E protein in viral infection: a potential target for LAV development and therapeutic strategies. *bioRxiv* https://doi.org/10.1101/2020.05.11.088781.
40. Dey, D., S. Borkotoky, and M. Banerjee. 2020. In silico identification of Tretinoin as a SARS-CoV-2 envelope (E) protein ion channel inhibitor. *Comput. Biol. Med.* 127:104063.
41. Kern, D. M., B. Sorum, …, S. G. Brohawn. 2020. Cryo-EM structure of the SARS-CoV-2 3a ion channel in lipid nanodiscs. *bioRxiv* https://doi.org/10.1101/2020.06.17.156554.
42. Richter, J. D., D. C. Evers, and L. D. Smith. 1983. The recruitment of membrane-bound mRNAs for translation in microinjected Xenopus oocytes. *J. Biol. Chem.* 258:2614–2620.
43. Chen, J., K. H. Lee, …, D. C. Wiley. 1998. Structure of the hemagglutinin precursor cleavage site, a determinant of influenza pathogenicity and the origin of the labile conformation. *Cell.* 95:409–417.
44. Anand, P., A. Puranik, …, V. Soundararajan. 2020. SARS-CoV-2 selectively mimics a cleavable peptide of human ENaC in a strategic hijack of host proteolytic machinery. *bioRxiv* https://doi.org/10.1101/2020.04.29.069476.
45. Kumar, A., P. Prasoon, …, K. Kant. 2021. SARS-CoV-2-specific virulence factors in COVID-19. *J. Med. Virol.* 93:1343–1350.
46. Gordon, D. E., J. Hiatt, …, N. J. Krogan; QCRG Structural Biology Consortium; Zoonomia Consortium. 2020. Comparative host-coronavirus protein interaction networks reveal pan-viral disease mechanisms. *Science.* 370:eabe9403.